DIAS
Institiúid Ard-Léinn Bhaile Átha Cliath | Dublin Institute for Advanced Studies

Chaos theory with a system of D0-branes.

Robert Kelly in collaboration with Cillian Kelly.
Supervisor: Dr. Swapnamay Mondal.

August 2, 2023

Contents

1 Abstract

This report investigates the classical limit of a quantum mechanical model of the dynamics of a system of D0-branes. The energy dependence of the Lyapunov exponent was found to be $\lambda_L(E) = (0.100 \pm 0.0077)E^{0.24\pm0.011}$ for the system of four D0-branes, and $\lambda_L(E) = (0.080 \pm 0.0025)E^{0.220\pm0.0059}$ for the system of seven D0-branes. To study what properties of a black hole this model retains in the classical limit, it was verified that the system is a fast scrambler using a classical analogue of the scrambling time t^* by showing that t^* scales as the log of the degrees of freedom, $t^* \sim ln(N^2)$.

2 Acknowledgments

I would like to thank my supervisor Dr. Swapnamay Mondal for providing the theoretical basis of string theory required for this project as well as invaluable guidance over the course of this research, and Dr. Saki Koizumi and Dr. Atri Dey for organising the studentship program and help with the creation of this report. I would also like to thank the staff at the Dublin Institute for Advanced Studies and students in the program for their great hospitality, stimulating discussions, and the welcoming atmosphere they provided.

3 Introduction and Theory

3.1 Chaos theory

This report deals with chaos theory in the framework of classical mechanics, which is a completely deterministic model of the dynamic evolution of systems. If all aspects of the system are completely known then the outcome, no matter how far in the future, is guaranteed if the system obeys classical mechanics. However in real world situations all properties of the system can never be completely accurately measured. Because of this, the rate at which two initially similar states of a system diverge as they evolve in time is an important property to study. A chaotic system experiences exponential divergence of its properties with time.

In a dynamical system that obeys ergodic theory, the system's average behavior over long periods of time equals its phase average [2]. If such a system is allowed to evolve for a long enough period of time from any arbitrary initial state, thermodynamic properties of the system can then be computed. The initial system under investigation here will therefore be thermalised for one thousand seconds before simulation measurements and observations will be made.

A black hole has temperature as can be derived from its Hawking radiation. It has also been conjectured that black holes are maximally chaotic systems in the sense that they are the fastest scramblers in nature [5]. Under string theory a set of D0-branes may be used to model a black hole. It is therefore of interest

to study if a system of D0-branes in the classical limit exhibits chaotic nature as well.

3.2 Lagrangian formalism

The endpoints of open strings are subject to either Dirichlet or Neumann boundary conditions in the nine spatial dimensions of sting theory. If an endpoint is subject Dirichlet boundary conditions in some dimension its position remains constant in that dimension while Neumann boundary conditions mean it is free to move along a hyperplane spanning those dimensions. These hyperplanes are called D-branes. D0-branes are point-like objects which do not allow the endpoints of any string attached to them to move as the endpoint obeys Dirichlet boundary conditions in all spatial dimensions. The D0-Branes themselves can move in space however and the chaotic nature of their dynamics is under investigation here.

In a system of N D0-branes close together, many types of open strings can be constructed, a string can have both endpoints on one D0-brane, or it can go from one D0-brane to any other. To quantify the possible string configurations, N $\times$ N matrices are required for each spatial dimension to capture the positions of the D0-branes along with the coupling of D0-branes together.

The Lagrangian of N D0-Branes under investigation given by Shenker et. al. [4] is the following:

$$L = \frac{1}{2g^2}\mathrm{Tr}(\sum_i [D_t X^i]^2) + \frac{1}{4g^2}\mathrm{Tr}(\sum_{j\neq i}[X^i, X^j]^2) + ... \tag{1}$$

$$X^i = \mathrm{N} \times \mathrm{N} \text{ Hermitian traceless matrix, i = 1,...,9.}$$

The other terms in the Lagrangian not explicitly written down here involve fermions and go to zero in the classical approximation which is taken in this report. g quantifies the coupling of the system and allows the coupling strength to be increased or decreased. In order to reach the classical approximation, a weak coupling/high temperature limit must be reached. This is because any quantum system in the high temperature limit is well approximated by its classical dynamics. Therefore g will be scaled as $g = 1/\sqrt{N}$ in the analysis. $D_t X^i = \partial_t X^i - [A_t, X^i]$ is the covariant derivative of X^i, with A_t being the $SU(\mathrm{N})$ gauge field we choose for the system. This is set to $A_t = 0$ for the analysis done here so that $[D_t X^i]^2 = [\partial_t X^i]^2 = [\dot{X}^i]^2$.

The Lagrangian equations of motion provide the dynamics of the system.

$$0 = \frac{d}{dt}(\frac{\partial L}{\partial \dot{X}^i}) - \frac{\partial L}{\partial X^i}.$$

$$\ddot{X}^i(t) = \sum_j [X^j, [X^i, X^j]]. \tag{2}$$

The equation of motion for the generalised coordinate A_t can also be found and leads to a constraint on the system known as the Gauss' law constraint [4].

$$0 = \frac{d}{dt}(\frac{\partial L}{\partial \dot{A}_t}) - \frac{\partial L}{\partial A_t}.$$
$$0 = \sum_i [X^i, \dot{X}^i]. \tag{3}$$

Derivations of equations (2) and (3) are available in the appendix.
The system is closed so total energy is conserved throughout the simulations:

$$E = \frac{1}{2g^2}\mathrm{Tr}(\sum_i [D_t X^i]^2) - \frac{1}{4g^2}\mathrm{Tr}(\sum_{j\neq i}[X^i, X^j]^2) + ... \tag{4}$$

The equipartition theorem is used to find the temperature of the system [4]:

$$E = \frac{3}{4} fT. \tag{5}$$

Where f is the number of degrees of freedom of the system. There are nine N^2 position matrices for this system so at first glance $f = 9N^2$. However these matrices are traceless which makes $f = 9(N^2 - 1)$ as you can find the final diagonal element of each matrix from subtracting the sum of the other diagonal elements. Gauss' law allows one matrix to be found from the other eight so $f = 8(N^2 - 1)$. Finally the total angular momentum of the system, $\mathrm{Tr}(X^i \dot{X}^j - X^j \dot{X}^i)$, is conserved lowering the degrees of freedom by $\sum_n^8 n$ making the final value for $f = 8(N^2 - 1) - 36$.

3.3 Perturbation

Once the system is thermalised, it must be perturbed while keeping the Gauss' law constraint. This is done by adding an extra term into the potential of the Lagrangian:

$$\mathrm{L} = \frac{1}{2g^2}\mathrm{Tr}(\sum_i [D_t X^i]^2) + \frac{1}{4g^2}\mathrm{Tr}(\sum_{j\neq i}[X^i, X^j]^2) + \sum_{k=1}^{2} k c_k \mathrm{Tr}(\sum_i [X^i]^2)$$

The coefficients c_k are randomly chosen from the Gaussian distribution with mean zero and standard deviation $\sigma = 10^{-8}$ which allow the perturbations to be both random and small. The equations of motion for this new Lagrangian are:

$$\ddot{X}^i = \sum_j [X^j, [X^i, X^j]] + \sum_{k=1}^{2} k c_k \{X^i, (\sum_j X_j^2)^{k-1}\}.$$

Here,{...} is the anti-commutator.

For k = 1; $(\sum_j X_j^2)^{k-1} = (\sum_j X_j^2)^0$ = Identity matrix. The identity matrix in an anti-commutator works as follows:

$$\{A, I\} = AI + IA = 2A.$$

Therefore the perturbation equation of motion is simplified to the following:

$$\ddot{X}^i = \sum_j [X^j, [X^i, X^j]] + 2c_1 X^i + 2c_2 \{X^i, (\sum_j X_j^2)\}. \tag{6}$$

3.4 Chaotic divergence

As discussed in section 3.1, a system is chaotic if the divergence of two initially similar states of the system is exponential. Let the distance between two states of the system with the same energy be defined as follows [4]:

$$|\delta X(t)| = \sqrt{\sum_i \mathrm{Tr}(X_1^i(t) - X_2^i(t))^2}. \tag{7}$$

X_1^i is the X^i position matrix of one state and X_2^i the position matrix of the other state. Then the chaotic behaviour of a system is defined by the following equation:

$$|\delta X(t)| = |\delta X(0)| e^{\lambda_L t}. \tag{8}$$

The Lyapunov exponent, λ_L, must be positive for the system to be chaotic. From equation (8), λ_L can be calculated as the slope of the graph of $ln(\frac{|\delta X(t)|}{|\delta X(0)|})$ against time t.

As the system in question has its total energy conserved, the phase space of all possible configurations of the system is bounded, which means that the two states cannot diverge for infinite time. They will diverge at a constant exponential rate defined by the Lyapunov exponent until such a time, t^*, where the perturbation is of the same order as the system size [4]. This t^* is the classical analogue of the scrambling time. $|\delta X(t)|$ for $t > t^*$ stays a constant

and cannot be used when λ_L is being calculated. Figure 1 shows a log scale graph of $|\delta X(t)|$ against time, displaying the scrambling time and the maximum distance the two states can be apart. Therefore, when calculating λ_L as the slope of $ln(\frac{|\delta X(t)|}{|\delta X(0)|})$ against t, only data points with $t < t^*$ may be used as the fact that $|\delta X(t)|$ converges to a maximum distance has nothing to do with the Lyapunov exponent but on the constraints of the system.

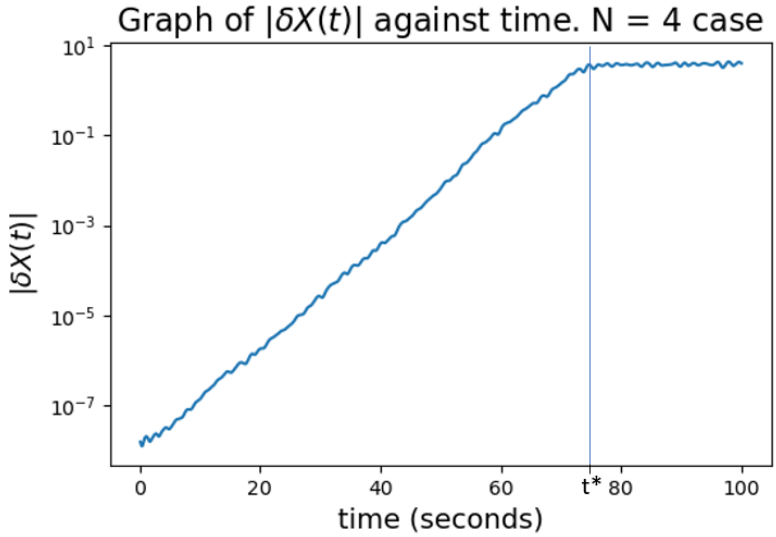

Figure 1: Example graph of distance against time for four D0-branes. The graph is linear and the y-axis is log-scaled, meaning that the distance has an exponential dependence on time. Exponential growth continues until the perturbation is of the same order as the system size at $t = t^*$ (scrambling time).

3.5 Fast scrambler

It has been conjectured that the upper bound for the rate at which a quantum system can scramble information is logarithmic in the degrees of freedom [7]. In quantum mechanics, to scramble information effectively means to alter an original system so that any information it contained can only be recovered by analysing at least half of the degrees of freedom. The time the system takes to do this is called the scrambling time t^*. Under this definition black holes are the fastest scramblers in nature [7]. It must be verified that the D0-brane system in question here still retains its fast scrambling behaviour in the classical limit and with the classical analogue of scrambling time which is the time it takes for $|\delta X(t)|$ to reach its maximum, t^*. In this system we have seen that the number of degrees of freedom is $f = 8(N^2 - 1) - 36$ which scales as N^2. Therefore we expect the following:

$$t^* \sim ln(N^2).$$
$$t^* \sim \frac{k}{2} ln(N^2) \tag{9}$$

For some constant k.

t^* is also the time it takes $ln(\frac{|\delta X(t)|}{|\delta X(0)|})$ to reach its maximum and λ_L is the slope of the linear graph of $ln(\frac{|\delta X(t)|}{|\delta X(0)|})$ against t. Decreasing the slope of a linear graph directly correlates with increasing the time it takes for the function to reach its maximum value. Therefore t^* is inversely dependent on λ_L. If the way in which λ_L scales is independent of N then this inverse dependence can be added to equation (9):

$$t^* \sim \frac{k}{2\lambda_L} ln(N^2)$$
$$\lambda_L t^* \sim \frac{k}{2} ln(N^2)$$

The above scaling rule can be expressed in terms of $|\delta X(t^*)|$ by using equation (8) and taking the exponential of both sides:

$$e^{\lambda_L t^*} \sim N^k$$
$$|\delta X(t^*)| \sim N^k$$
$$\frac{|\delta X(t^*)|}{N^k} = \text{constant} \tag{10}$$

In order to determine if the system of D0-branes is a fast scrambler, equation (10) is tested in this report for multiple values of N. It must also be verified that the λ_L is indeed independent of N in order for equation (10) to be valid.

4 Method

4.1 Simulating the dynamic evolution of D0-branes

Numerical algorithms are usually necessary in dynamical simulations as there are most likely large amounts of objects being simulated. This makes analytical solutions to their equations of motion impossible. The numerical integration velocity Verlet algorithm is used to determine the values of $X(t + \Delta t)$ and $\dot{X}(t+\Delta t)$ [3]. This gives insight into the time dependent dynamics of this system. The dynamics of the simulated phase space will be obtained by numerically solving Lagrange's equations of motion.

$$X(t+\Delta t) = X(t) + \dot{X}(t)\Delta t + \frac{1}{2}\ddot{X}(t)\Delta t^2. \tag{11}$$

$$\dot{X}(t+\Delta t) = \dot{X}(t) + \frac{1}{2}(\ddot{X}(t) + \ddot{X}(t+\Delta t))\Delta t. \tag{12}$$

Equations (11) and (12) are the numerical integration equations needed to perform the velocity Verlet algorithm and allow us to calculate X^i and $\dot{X}^i$ from only the information of the previous time step or our initial conditions. The derivation of equations (11) and (12) is given in the appendix. Using these equations and the equations of motion, the dynamics of the system can now be numerically solved using the velocity Verlet algorithm:

- Set initial position ($X^i(t)$) and velocity ($\dot{X}^i(t)$) matrices for the system.
- Use equation (2) to calculate the initial acceleration ($\ddot{X}^i(t)$) matrices.
- Use equation (11) to calculate $X^i(t+\Delta t)$.
- Calculate $\ddot{X}^i(t+\Delta t)$ using equation (2).
- Use equation (12) to calculate $\dot{X}^i(t+\Delta t)$.
- Define $X^i(t+\Delta t)$, $\dot{X}^i(t+\Delta t)$, and $\ddot{X}^i(t+\Delta t)$ as $X^i(t)$, $\dot{X}^i(t)$, and $\ddot{X}^i(t)$ respectively.
- Repeat the previous four steps, increasing the time by Δt each iteration.

Δt was set to 10^-4 seconds for all simulations. The elements of the initial velocity matrices were set to $\dot{X}^i_{ij}(0) = 0$ for all i so that the total momentum of the system would be set to zero and conserved throughout the simulation. $X^i(0)$ were random N $\times$ N Hermitian traceless matrices. The diagonal elements of these matrices were real numbers as the matrices were Hermitian and were created by sampling from a Gaussian distribution with mean of zero and standard deviation σ, i.e. $X^i_{ii}(0) \sim N(0,\sigma)$. To make $X^i(0)$ traceless, $X^i_{NN}(0) = -\sum_i^{N-1} X^i_{ii}(0)$. Finally the off-diagonal complex elements had their real and imaginary parts sampled from the same Gaussian distribution $N(0,\sigma)$. In order to change the total energy (E) of the system, σ was increased or decreased until $X^i(0)$ gave an E within ± 0.01 of the required value by equation (4).

The initial system was thermalised for one thousand seconds so that a typical state was reached using the velocity Verlet algorithm. This stopped any atypical behaviour being recorded as a result of the arbitrary initial conditions used to start the simulation. Starting from these thermalised coordinates, a perturbed state was reached by swapping out equation (2) for equation (6) in the algorithm and evolving the simulation for one second. Equation (2) was replaced back into the algorithm and the original thermalised state was evolved for one second, thus giving two initially very similar states. These are the states described by $X^i_1(t)$

and $X_2^i(t)$ in equation (7). If the Lyapunov exponents for the N = 4 and N = 7 cases are very similar for the same energy, then the Lyapunov exponent can be said to be independent of N to leading order which is necessary for the reasoning in section 3.5 to hold.

4.2 Lyapunov exponent

In order to check the chaotic nature of the system both $X_1^i(t)$ and $X_2^i(t)$ were evolved for 100 seconds and all X^i were recorded every 0.1 seconds. For these recorded values the distance between both states was calculated using equation (7) so that the exponential increase of this distance may be verified. If the scrambling time was found to be ninety seconds or above then the simulation was instead run for one hundred and fifty seconds so that the maximum distance was certainly reached.

In order to analyse the energy dependence on the Lyapunov exponent, six simulations were run for the N = 4 case with E = 63, 157.5, 315, 630, 1260, and 1890 respectively. Another four simulations were run for the N = 7 case with E = 26.1, 130.5, 195.75, and 522 respectively.

4.3 Fast scrambler

In order to test if the system is a fast scrambler, three simulations for N = 8, 12, and 16 were performed. The initial perturbations $|\delta X(0)|$ were made constant for these three simulations and the systems all had the same temperature T = 1 so that the difference in scrambling time was entirely because of the change in N. These simulations were also used to compare the methodology used in this report to other literature values of the Lyapunov exponent in this system.

5 Results

5.1 Lyapunov exponent

This report has found good agreement of the value of the Lyapunov exponent with other work on the same system. For example the following equation for the Lyapunov exponents from similar simulation runs has been found:

$$\lambda_L = (0.29252 - \frac{0.424}{N^2})(g^2 NT)^{\frac{1}{4}}. \text{ (Shenker et. al. [4])}$$

Comparing simulation runs with $T = 1$ and $g^2 N = 1$ to results from this equation give the following results.

Case	*Equation*	*Experiment*
$N = 8$	$\lambda_L = 0.2853$	$\lambda_L = 0.2865$
$N = 12$	$\lambda_L = 0.2891$	$\lambda_L = 0.2893$
$N = 16$	$\lambda_L = 0.2903$	$\lambda_L = 0.2884$

For each simulation, the graph of $|\delta X(t)|$ was plotted against time t in order to find the scrambling time for the system. Such a graph for the N = 4 case with various energies is presented in figure 2. This graph displays that the maximum distance $|\delta X(t^*)|$ was very similar for all simulations, ranging from 4 to 9 overall, meaning that $|\delta X(t^*)|$ has at most a small dependence on the energy of the system. It is also clear that the initial distances are not the same for each experimental run as the data sets do not line up at $t = 0$. This is because the perturbations were random as discussed in section 3.3 so $|\delta X(0)|$ was random too. This is not important however as the slopes of these graphs are not affected by $|\delta X(0)|$.

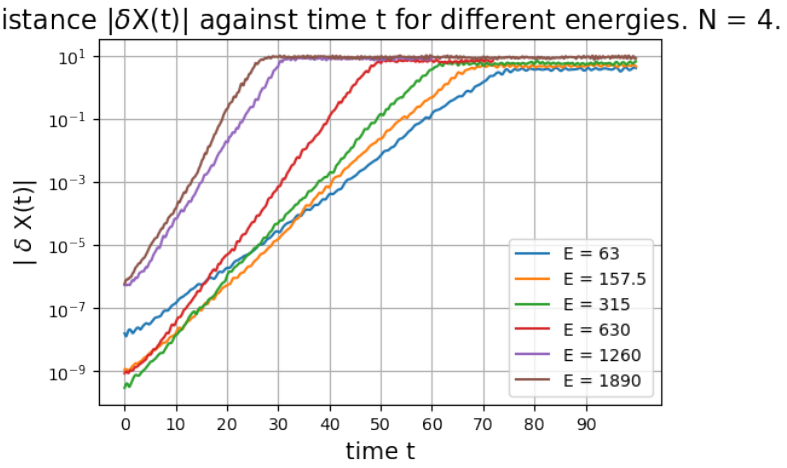

Figure 2: Graph of $|\delta X(t)|$ against time for multiple total energies of four D0-branes. Exponential growth continues until the perturbation is of the same order as the system size. $|\delta X(t^*)|$ is roughly the same for all simulations.

The relationship between λ_L and energy is more readily seen once the data sets are rescaled to start at zero by plotting $ln(\frac{|\delta X(t)|}{|\delta X(0)|})$ against time in figure 3. The Lyapunov exponent equals the slope of each data set before t^* is reached. It is clear from figure 3 that the higher the energy of the system, the steeper the slope and the greater the Lyapunov exponent.

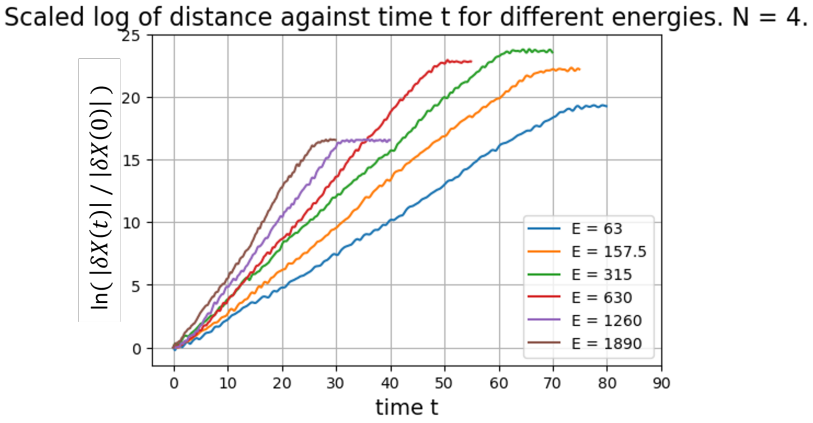

Figure 3: Graph of $ln(\frac{|\delta X(t)|}{|\delta X(0)|})$ against time for multiple total energies of four D0-branes. The slope of the data set equals the Lyapunov exponent for that simulation. Exponential growth continues until the perturbation is of the same order as the system size. The increase in the slope of each data set correlates with the increase in energy of the system.

It was found that the Lyapunov exponent does depend on the total energy of the system E. Figure 4 displays this relation for the N = 4 case.

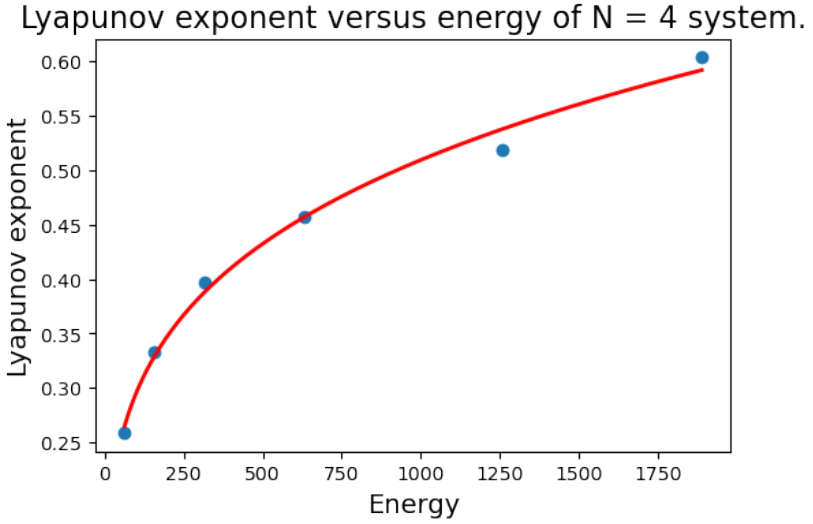

Figure 4: Graph of the Lyapunov exponent against total energy of the system for the N = 4 case. $\lambda_L(E) \propto E^{0.24}$.

Similar analysis was done for the system of seven D0-branes, leading to figure

5 which displays the same kind of dependence of λ_L on E.

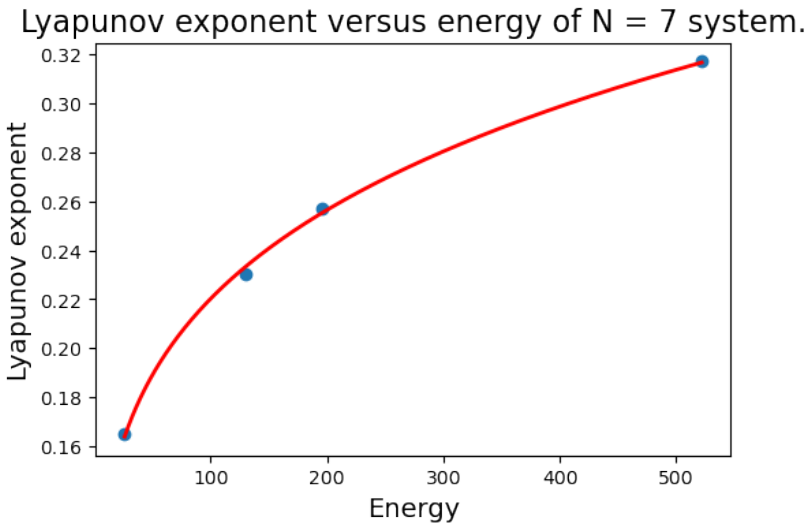

Figure 5: Graph of the Lyapunov exponent against total energy of the system for the N = 7 case. $\lambda_L(E) \propto E^{0.220}$.

The curves of best fit for figures 4 and 5 are as follows:

$$\lambda_L(E) = (0.100 \pm 0.0077)E^{0.24\pm0.011} \tag{13}$$

$$\lambda_L(E) = (0.080 \pm 0.0025)E^{0.220\pm0.0059} \tag{14}$$

for the N = 4 and N = 7 case respectively. These equations show that λ_L scales as $E^0.24$ for these simulation runs.

5.2 Fast scrambler

Equation (10) sets out the relationship that is expected of a fast scrambling system. It is expected that the graph of $\frac{|\delta X(t)|}{N^k}$ against time for some particular value of k should reach the same maximum value for all N. In order to test this, three simulations were performed for N = 8, 12, and 16. Empirically it was found that for this system of D0-branes, $k = \frac{1}{2}$. The graph of $\frac{|\delta X(t)|}{\sqrt{N}}$ for the three simulations is displayed in figure 6. All three data sets have the same maximum distance $\frac{|\delta X(t^*)|}{\sqrt{N}}$ = constant which is the relationship predicted by equation (10).

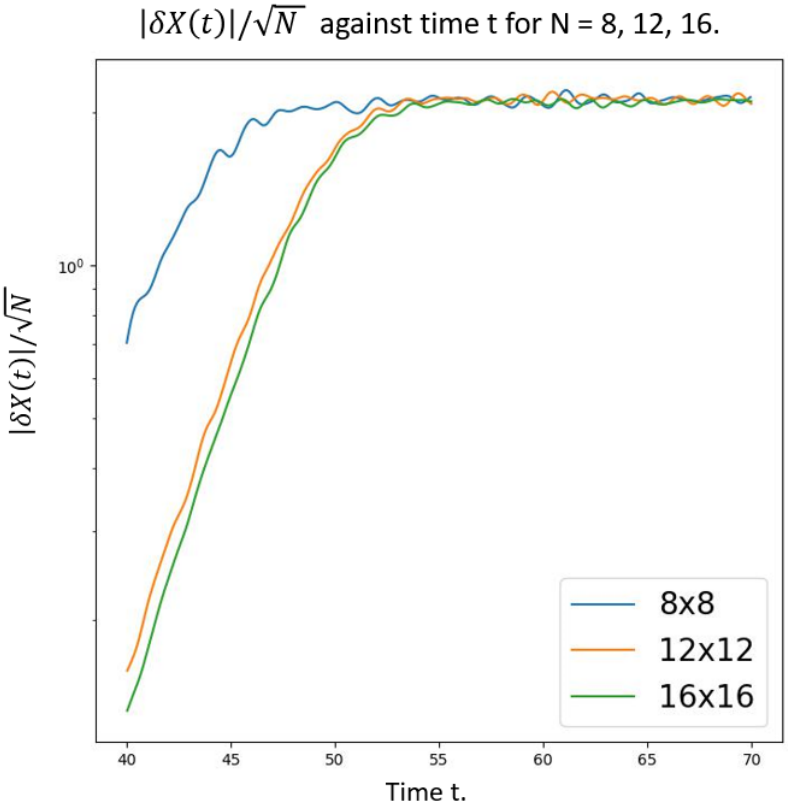

Figure 6: Graph of $\frac{|\delta X(t)|}{\sqrt{N}}$ against t for N = 8, 12, and 16. .

By the reasoning in section 3.5 this result shows that the scrambling time does indeed scale as $ln(N^2)$ or as the logarithm of the degrees of freedom of the system. This shows that the system of D0-branes still retains the fast scrambling property of a black hole in the classical limit.

5.3 Error analysis

The errors presented for equations (13) and (14) are an underestimate as they only represent the error in the linear least squares curves of best fit assuming the data points are completely accurate which is not true. They do not take into account the statistical inaccuracies brought into the simulations due to numerical integration techniques.

Errors are always present in simulations by the fact that we numerically integrate the equations of motion. The velocity Verlet equations are derived by truncating the Taylor expansion of X(t) and this truncation means that the values we get from using this algorithm will never be completely accurate. In the derivation of the velocity Verlet equations in the appendix, adding equations

(22) and (23) cancels out the third order terms in the Taylor expansions, meaning we only need to truncate the expansions at the fourth order. This makes the local error of the velocity Verlet equations $\mathcal{O}(\Delta t^4)$. The global error from the velocity Verlet equations is however $\mathcal{O}(\Delta t^2)$ as the error from one iteration accumulates with the error from the next. Therefore in practice, this is a second order integrator. Using a small time step of $\Delta t = 10^{-4}$ throughout simulations reduces the size of this error. Decreasing the step size more would reduce this error but was deemed too computationally intensive for this project.

A method of analysing error introduced by the numerical integration is to check the conservation of energy throughout a simulation run. This was done by calculating the total energy of the system from equation (4) every second. A graph of total energy against time is displayed in figure 7, where it is seen that over one hundred seconds the system's energy was conserved to seven significant figures. There are no trends in the graph which shows that although the numerical errors were accumulating over time as in all numerical simulations, they did not get large enough over the course of the simulation to skew the total energy. This suggests that the errors were small and the step size chosen was adequate.

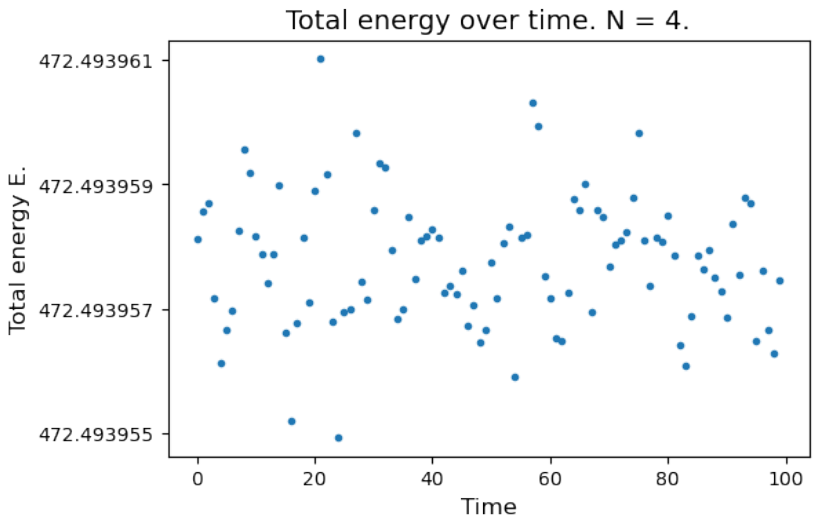

Figure 7: Graph of total system energy over time for a simulation with temperature T = 7.5 and N = 4. The total energy is conserved to seven significant figures throughout the one hundred second simulation, and there are no trends in the graph.

6 Discussion

The close agreement of Lyapunov exponents obtained here to those produced elsewhere [4] provides a good level of confidence in the methodology employed. This gives more weight to the other results presented here. Equations (13) and (14) display that λ_L scales as $E^{0.24\pm0.011}$ for N = 4 and $E^{0.220\pm0.0059}$ for N = 7. The two exponents are not within error of each other, however the errors presented are underestimates as explained in section 5.3. Therefore the way in which λ_L scales with E does not depend on N to leading order. This is necessary for equation (10) to be valid as explained in section 3.5. The energy dependence of λ_L in this system also obeys a conjecture that the energy dependence of the Lyapunov exponent in any chaotic system is at most linear in the high energy limit [6]. In other words, the conjecture is that $\lambda_L(E) \propto E^c(E \to \infty)$, $c \leq 1$ which holds for this system. Figures 4 and 5 exemplify this relationship as the curve of best fit increases slower than a linear relationship would.

From section 3.5 and figure 6, the system is now known to be a fast scrambler. This shows that the system of D0-branes analysed here still retains this property of a black hole even in the classical limit. There are string theoretic models of black holes using D2- and D6-branes, further research is required to analyse if these models also have chaotic nature and have Lyapunov exponents with particular energy dependences.

7 Summary

The system of N D0-branes who's dynamics are governed by equation (1) is found to be a chaotic system as the divergence of similar initial states grows exponentially. The energy dependence of the Lyapunov exponent was found to be

$$\lambda_L(E) = (0.100 \pm 0.0077)E^{0.24\pm0.011}$$
$$\lambda_L(E) = (0.080 \pm 0.0025)E^{0.220\pm0.0059}$$

for the case of N = 4 and N = 7 respectively. Further research is required to analyse the energy dependence of the Lyapunov exponent for other values of N.

Figure 6 displays that the classical analogue of scrambling time, t^* has been found to scale as the logarithm of the degrees of freedom of the system. This shows that the system of D0-branes modelled here is a fast scrambler.

8 Appendix

8.1 Derivation of equations of motion

The Lagrangian equations of motion are calculated as follows:

$$
\begin{aligned}
0 &= \frac{d}{dt}(\frac{\partial L}{\partial \dot{X}^k}) - \frac{\partial L}{\partial X^k}. \\
\frac{d}{dt}(\frac{\partial L}{\partial \dot{X}^k}) &= \frac{d}{dt}(\frac{\partial_{\frac{1}{2g^2}} \mathrm{Tr}(\sum_i [D_t X^i]^2)}{\partial \dot{X}^k}). \\
&= \frac{1}{2g^2}\frac{d}{dt}(\frac{\partial \mathrm{Tr}(\sum_i [\dot{X}^i]^2)}{\partial \dot{X}^k}). \\
&= \frac{1}{2g^2}\frac{d}{dt}(2\dot{X}^{kT}) \\
&= \frac{1}{g^2}(\ddot{X}^{kT}). \qquad (15)
\end{aligned}
$$

Next calculate the derivative of the Lagrangian with respect to X^k:

$$
\begin{aligned}
\frac{\partial L}{\partial X^k} &= \frac{\partial}{\partial X^k}(\frac{1}{4g^2}\mathrm{Tr}(\sum_{j\neq i}[X^i, X^j]^2)). \\
&= \frac{1}{4g^2}\frac{\partial}{\partial X^k}(\mathrm{Tr}(\sum_i [X^i, X^k]^2 + \sum_j [X^k, X^j]^2)). \\
&= \frac{1}{2g^2}\frac{\partial}{\partial X^k}(\mathrm{Tr}(\sum_i [X^i, X^k]^2)). \\
&= \frac{1}{2g^2}\frac{\partial}{\partial X^k}(\sum_i \mathrm{Tr}([X^i X^k - X^k X^i][X^i X^k - X^k X^i])). \\
&= \frac{1}{2g^2}\frac{\partial}{\partial X^k}(\sum_i \mathrm{Tr}(X^k[X^i X^k - X^k X^i]X^i) - \mathrm{Tr}(X^k X^i[X^i X^k - X^k X^i])). \\
&= \frac{1}{2g^2}\frac{\partial}{\partial X^k}(\sum_i \mathrm{Tr}(2X^k X^i X^k X^i - 2X^k X^k X^i X^i)). \\
&= \frac{1}{2g^2}\frac{\partial}{\partial X^k}(\sum_i 2\mathrm{Tr}(X^k X^i X^k X^i - X^k X^k X^i X^i)). \\
&= \frac{1}{g^2}\sum_i (2(X^i X^k X^i)^T - (X^k X^i X^i)^T - (X^i X^i X^k)). \\
&= \frac{1}{g^2}\sum_i ([X^i, X^k]X^i - X^i[X^i, X^i])^T. \\
&= \frac{1}{g^2}\sum_i [[X^i, X^k], X^i]^T. \\
&= -\frac{1}{g^2}\sum_i [X^i, [X^i, X^k]]^T. \\
&= \frac{1}{g^2}\sum_i [X^i, [X^k, X^i]]^T. \qquad (16)
\end{aligned}
$$

Substitute equations (15) and (16) into the equations of motion, take the transpose of both sides, and then swap the dummy variables k for i and i for j:

$$\begin{aligned}
0 &= \frac{1}{g^2}\ddot{X}^{kT} - \frac{1}{g^2}\sum_i [X^i,[X^k,X^i]]^T. \\
0 &= \ddot{X}^{kT} - \sum_i [X^i,[X^k,X^i]]^T. \\
\ddot{X}^{kT} &= \sum_i [X^i,[X^k,X^i]]^T. \\
\ddot{X}^{i} &= \sum_j [X^j,[X^i,X^j]].
\end{aligned} \tag{17}$$

8.2 Derivation of Gauss' Law

The equation of motion for the generalised coordinate A_t can be found and leads to the Gauss' law constraint. There is no dependence on $\dot{A}_t$ so the first term in the equation of motion is zero.

$$\begin{aligned}
0 &= \frac{d}{dt}\left(\frac{\partial L}{\partial \dot{A}_t}\right) - \frac{\partial L}{\partial A_t}. \\
0 &= -\frac{\partial L}{\partial A_t}. \\
0 &= -\frac{1}{2g^2}\frac{\partial \mathrm{Tr}(\sum_i [D_t X^i]^2)}{\partial A_t}. \\
0 &= -\frac{1}{2g^2}\frac{\partial \mathrm{Tr}(\sum_i (\dot{X}^i - [A_t,X^i])^2)}{\partial A_t}.
\end{aligned} \tag{18}$$

$$\begin{aligned}
\mathrm{Tr}(\sum_i (\dot{X}^i - [A_t,X^i])^2) =& \mathrm{Tr}(\sum_i \dot{X}^{i2}) - \mathrm{Tr}(\sum_i A_t X^i A_t X^i) \\
&+ \mathrm{Tr}(\sum_i X^i A_t X^i A_t) - \mathrm{Tr}(\sum_i \dot{X}^i A_t X^i) \\
&- \mathrm{Tr}(\sum_i A_t X^i \dot{X}^i) + \mathrm{Tr}(\sum_i \dot{X}^i X^i A_t) \\
&+ \mathrm{Tr}(\sum_i X^i A_t \dot{X}^i) - \mathrm{Tr}(\sum_i A_t X^i X^i A_t) \\
&- \mathrm{Tr}(\sum_i X^i A_t A_t X^i).
\end{aligned} \tag{19}$$

Since Tr(ABC) = Tr(CAB) = Tr(BCA), many terms cancel and add together in the above equation and the commutator of X^i and $\dot{X}^i$ appears:

$$
\begin{aligned}
(19) =& \mathrm{Tr}(\sum_i \dot{X}^{i2}) - 2\mathrm{Tr}(\sum_i \dot{X}^i A_t X^i) + 2\mathrm{Tr}(\sum_i \dot{X}^i X^i A_t) - 2\mathrm{Tr}(\sum_i A_t X^i X^i A_t). \\
(19) =& \mathrm{Tr}(\sum_i \dot{X}^{i2}) - 2\mathrm{Tr}(A_t \sum_i X^i \dot{X}^i) + 2\mathrm{Tr}(A_t \sum_i \dot{X}^i X^i) - 2\mathrm{Tr}(A_t^2 \sum_i X^{i2}). \\
(19) =& \mathrm{Tr}(\sum_i \dot{X}^{i2}) - 2\mathrm{Tr}(A_t \sum_i [X^i, \dot{X}^i]) - 2\mathrm{Tr}(A_t^2 \sum_i X^{i2}). \qquad (20)
\end{aligned}
$$

Plug equation (20) into equation (18) and solve the derivatives:

$$
\begin{aligned}
0 &= -\frac{1}{2g^2}\frac{\partial}{\partial A_t}(\mathrm{Tr}(\sum_i \dot{X}^{i2}) - 2\mathrm{Tr}(A_t \sum_i [X^i, \dot{X}^i]) - 2\mathrm{Tr}(A_t^2 \sum_i X^{i2})). \\
0 &= \frac{1}{g^2}\frac{\partial}{\partial A_t}(\mathrm{Tr}(A_t \sum_i [X^i, \dot{X}^i]) + \mathrm{Tr}(A_t^2 \sum_i X^{i2})). \\
0 &= \frac{1}{g^2}((\sum_i [X^i, \dot{X}^i])^T + (A_t \sum_i X^{i2} + \sum_i X^{i2} A_t)).
\end{aligned} \qquad (21)
$$

Let $A_t = 0$ and Gauss' law is found.

$$
\begin{aligned}
0 &= \frac{1}{g^2}(\sum_i [X^i, \dot{X}^i])^T. \\
0 &= (\sum_i [X^i, \dot{X}^i])^T. \\
0 &= \sum_i [X^i, \dot{X}^i].
\end{aligned}
$$

8.3 Derivation of velocity Verlet algorithm

To derive the velocity Verlet algorithm, the position X is Taylor expanded about the time point t [3]:

$$X(t + \Delta t) = X(t) + \dot{X}(t)\Delta t + \frac{1}{2}\ddot{X}(t)\Delta t^2 + \frac{1}{6}\frac{d\ddot{X}(t)}{dt}\Delta t^3 + \mathcal{O}(\Delta t^4). \qquad (22)$$

$$X(t - \Delta t) = X(t) - \dot{X}(t)\Delta t + \frac{1}{2}\ddot{X}(t)\Delta t^2 - \frac{1}{6}\frac{d\ddot{X}(t)}{dt}\Delta t^3 + \mathcal{O}(\Delta t^4). \qquad (23)$$

Equation (22) and (23) are added together and the first and third order terms cancel:

$$X(t+\Delta t) + X(t-\Delta t) = 2X(t) + \ddot{X}(t)\Delta t^2 + \mathcal{O}(\Delta t^4).$$
$$X(t+\Delta t) = 2X(t) - X(t-\Delta t) + \ddot{X}(t)\Delta t^2 + \mathcal{O}(\Delta t^4). \quad (24)$$

Equation (24) is the Verlet algorithm and can be used to calculate the new position from old variables. However it requires knowing the position $X(t-\Delta t)$ which is not possible at the start of the simulation. To improve on this, the velocity Verlet algorithm [3] will be used in this report. The velocity Verlet algorithm is derived by subtracting equation (23) from (22), and solving for $X(t-\Delta t)$:

$$X(t+\Delta t) - X(t-\Delta t) = 2\dot{X}(t)\Delta t + \mathcal{O}(\Delta t^3). \quad (25)$$
$$X(t-\Delta t) = X(t+\Delta t) - 2\dot{X}(t)\Delta t. \quad (26)$$

Substitute equation (26) into the Verlet algorithm, equation (24), and solve for $X(t+\Delta t)$:

$$X(t+\Delta t) = 2X(t) - [X(t+\Delta t) - 2\dot{X}(t)\Delta t] + \ddot{X}(t)\Delta t^2.$$
$$X(t+\Delta t) = X(t) + \dot{X}(t)\Delta t + \frac{1}{2}\ddot{X}(t)\Delta t^2. \quad (27)$$

We then solve equation (25) for $\dot{X}(t)$, and substitute equation (24) into it:

$$\dot{X}(t) = \frac{X(t+\Delta t) - X(t-\Delta t)}{2\Delta t}.$$
$$\dot{X}(t) = \frac{[2X(t) - X(t-\Delta t) + \ddot{X}(t)\Delta t^2] - X(t-\Delta t)}{2\Delta t}.$$
$$\dot{X}(t) = \frac{X(t) - X(t-\Delta t)}{\Delta t} + \frac{1}{2}\ddot{X}(t)\Delta t. \quad (28)$$

Finally increase the time of equation (28) by Δt and substitute equation (27) into it:

$$\dot{X}(t+\Delta t) = \frac{X(t+\Delta t) - X(t)}{\Delta t} + \frac{1}{2}\ddot{X}(t+\Delta t)\Delta t.$$
$$\dot{X}(t+\Delta t) = \frac{[X(t) + \dot{X}(t)\Delta t + \frac{1}{2}\ddot{X}(t)\Delta t^2] - X(t)}{\Delta t} + \frac{1}{2}\ddot{X}(t+\Delta t)\Delta t.$$
$$\dot{X}(t+\Delta t) = \dot{X}(t) + \frac{1}{2}(\ddot{X}(t) + \ddot{X}(t+\Delta t))\Delta t. \quad (29)$$

Equations (27) and (29) make up the velocity Verlet algorithm.

9 References

[1] Petersen, K. (1983). Ergodic Theory. *Cambridge University Press*. pp.3-4.

[2] Moore, C. (2015). Ergodic theorem, ergodic theory, and statistical mechanics. *Proceedings of the National Academy of Sciences of the United States of America*. 112(7), pp.1907–1911.

[3] Frenkel, D. Berend Smit, B. (2002). Understanding Molecular Simulation from Algorithms to Applications 2nd Ed Chapter 4. *Academic Press*. pp.63-107.

[4] Gur-Ari, G. Hanada, M. Shenker, S. (2016). Chaos in Classical D0-Brane Mechanics. *Journal of High Energy Physics*. 91(2016).

[5] Savvidy, G. (2020). Maximally chaotic dynamical systems. *Annals of Physics*. 421.

[6] Hashimoto, K. Murata, K. Tanahashi, N. Watanabe, R. (2022). A bound on energy dependence of chaos. *Phys. Rev. D*. 106(12).
[7] Sekino, Y. Susskind, L. (2008). Fast Scramblers. *Journal of High Energy Physics*. 2008(10), p.65.